




Article

# Second Order Nonlinear Optical Properties of 4-Styrylpyridines Axially Coordinated to A<sub>4</sub> Zn<sup>II</sup> Porphyrins: A Comparative Experimental and Theoretical Investigation †

Francesca Tessore <sup>1</sup>, Gabriele Di Carlo <sup>1,\*</sup>, Alessandra Forni <sup>2</sup>, Stefania Righetto <sup>1</sup>,  
Francesca Limosani <sup>3,4</sup> and Alessio Orbelli Biroli <sup>2,5</sup>

<sup>1</sup> Department of Chemistry, University of Milan, INSTM Research Unit, Via C. Golgi 19, 20133 Milan, Italy; francesca.tessore@unimi.it (F.T.); stefania.righetto@unimi.it (S.R.)

<sup>2</sup> CNR-SCITEC, Istituto di Scienze e Tecnologie Chimiche “G. Natta”, c/o University of Milan, Via C. Golgi 19, 20133 Milan, Italy; alessandra.forni@scitec.cnr.it (A.F.); alessio.orbellibiroli@unipv.it (A.O.B.)

<sup>3</sup> Fusion and Nuclear Security Department, Photonics Micro and Nanostructures Laboratory, ENEA, Via E. Fermi 45, 00044 Frascati, Rome, Italy; francescalim@hotmail.it

<sup>4</sup> Department of Chemical Science and Technologies, University of Rome Tor Vergata, Via della Ricerca Scientifica 1, 00133 Rome, Italy

<sup>5</sup> Department of Chemistry, University of Pavia, Via Taramelli 12, 27100 Pavia, Italy

\* Correspondence: gabriele.dicarlo@unimi.it

† This paper is dedicated to Prof. Maddalena Pizzotti for her 70th birthday, and for her scientific contribution in the field of porphyrin chemistry.

Received: 13 July 2020; Accepted: 12 August 2020; Published: 14 August 2020



**Abstract:** In this research, two 4-styrylpyridines carrying an acceptor –NO<sub>2</sub> (L1) or a donor –NMe<sub>2</sub> group (L2) were axially coordinated to A<sub>4</sub> Zn<sup>II</sup> porphyrins displaying in 5,10,15,20 *meso* position aryl moieties with remarkable electron withdrawing properties (pentafluorophenyl (TFP)), and with moderate to strong electron donor properties (phenyl (TPP) < 3,5-di-*tert*-butylphenyl (TBP) < bis(4-*tert*-butylphenyl)aniline) (TNP)). The second order nonlinear optical (NLO) properties of the resulting complexes were measured in CHCl<sub>3</sub> solution by the Electric-Field-Induced Second Harmonic generation technique, and the quadratic hyperpolarizabilities β<sub>λ</sub> were compared to the Density Functional Theory (DFT)-calculated scalar quantities β<sub>||</sub>. Our combined experimental and theoretical approach shows that different interactions are involved in the NLO response of L1- and L2-substituted A<sub>4</sub> Zn<sup>II</sup> porphyrins, suggesting a role of backdonation-type mechanisms in the determination of the negative sign of Electric-Field-Induced Second Harmonic generation (EFISH) β<sub>λ</sub>, and a not negligible third order contribution for L1-carrying complexes.

**Keywords:** 4-styrylpyridine; Zn<sup>II</sup> porphyrins; axial coordination; nonlinear optics; EFISH; DFT calculations

## 1. Introduction

Since the beginning of the nineties, organometallic and coordination compounds have been extensively studied as chromophores for second order nonlinear optical (NLO) applications. Indeed, the introduction of a metal fragment in an organic environment allows a fine-tuning of its electronic properties [1]. By changing the electronic configuration, the oxidation state and the coordination sphere of the metal, new charge transfer (CT) transitions at low energy between the metal and the ligand (such as ligand-to-metal, LMCT, or metal-to-ligand, MLCT) can occur, enhancing the NLO response [2,3]. A topic of considerable investigation has been the effect of the coordination to a metal center on the

second order NLO properties of  $\pi$ -delocalized nitrogen-donor push–pull monodentate and chelating polydentate ligands (such as pyridines [4], bipyridines [5], phenanthrolines [6], and terpyridines [7,8]). In particular, when the metal center is  $Zn^{II}$ , a remarkable enhancement of the second order NLO response is recorded due to its inductive acceptor strength and its Lewis acid properties [5–8].

4-styrylpyridines have been coordinated to a variety of metal fragments, including carbonyl moieties [4,9] and metal carbonyl clusters [10]. Through coordination, the modulus of their quadratic hyperpolarizability  $\beta$  (which is the figure of merit of the second order NLO response) increases significantly, with a sign that depends on the nature of the substituent in *para* position. Electron donor groups lead to positive values, since the second order NLO response is dominated by an intraligand CT transition (ILCT), whereas electron acceptors result in a negative sign, due to the predominance of a MLCT transition [4,9].

Indeed, according to the “two-level” model developed by Oudar [11,12], the dipolar contribution to the quadratic hyperpolarizability  $\beta$  of a molecule depends on the electronic CT transitions of mobile polarizable electrons. Assuming that only one major CT dominates the second order NLO response, the component of the tensor  $\beta$  along the CT direction ( $\beta_{CT}$ ) is (Equation (1)):

$$\beta_{CT} = \frac{3}{2h^2c^2} \frac{v_{eg}^2 r_{eg}^2 \Delta\mu_{eg}}{(v_{eg}^2 - v_L^2)(v_{eg}^2 - 4v_L^2)}, \quad (1)$$

where  $v_{eg}$  is the frequency of the CT transition,  $r_{eg}$  the transition dipole moment,  $\Delta\mu_{eg}$  the difference between the excited and the ground state dipole moments, and  $v_L$  the frequency of the incident radiation. Since all the terms in Equation (1) are positive, the sign of  $\beta_{CT}$  is related to that of  $\Delta\mu_{eg}$ , which depends on the  $\beta$ -dictating CT transition [9]. A useful way to evaluate  $\beta_{CT}$  is solvatochromism [13].

The NLO response of porphyrin-based chromophores has been extensively investigated surveying traditional substitution patterns as for *meso* [14–18] and  $\beta$ -pyrrolic [19–21] push–pull arranged systems. The substituents position, the effect of the central metal atom, the solvent acidity, and the influence of aggregates formation have been thoroughly studied in such systems. On the contrary, the NLO properties of axially coordinated metal-porphyrins with both electron-donating and electron-accepting ligands have been only roughly investigated. Although some studies on electronic properties of axially coordinated  $A_4$   $Zn^{II}$  porphyrins were reported [22–24], only the effect of the coordination of 4-styrylpyridines carrying a  $-NMe_2$  donor or a  $-CF_3$  acceptor group to the axial position of  $Zn^{II}$ ,  $Ru^{II}$ , and  $Os^{II}$  5,10,15,20-Tetraphenylporphyrin (TPP) complexes was investigated for NLO purpose [25], with the latter being SHG-inactive due to the presence of a center of symmetry, which is lost by axial coordination. The lack of the expected increase of the  $\beta$  modulus of the ligand upon coordination was attributed to a noticeable axial  $\pi$ -backdonation from the  $d_{\pi}$  orbitals of the metal to the  $\pi^*$  antibonding orbitals of the pyridine ligand, which is opposite to the  $\sigma$ -donation from the pyridine nitrogen atom to the metal [26]. Furthermore, for coordination of both 4-styrylpyridines to  $ZnTPP$ , the solvatochromic investigation provided a negative value of  $\Delta\mu_{eg}$ , and therefore of  $\beta_{CT}$ , in contrast with the positive  $\beta_{1907}$  experimentally measured by the Electric-Field-Induced Second Harmonic generation (EFISH) technique [27,28]. However, the paper did not fully address this discrepancy and did not provide any theoretical support to the experimental data.

The EFISH technique allows the determination of the quadratic hyperpolarizability through Equation (2):

$$\gamma_{EFISH} = \mu_0 \beta_{\lambda}(-2\omega; \omega, \omega)/5kT + \gamma(-2\omega; \omega, \omega, 0). \quad (2)$$

$\mu_0 \beta_{\lambda}(-2\omega; \omega, \omega)/5kT$  is a quadratic dipolar orientational contribution in which  $\mu_0$  is the ground state molecular dipole moment and  $\beta_{\lambda}$  is the projection along the dipole moment direction of the vectorial component  $\beta_{vec}$  of the quadratic hyperpolarizability tensor working at an incident wavelength  $\lambda$ .  $\gamma(-2\omega; \omega, \omega, 0)$  is a purely electronic cubic contribution that is a third order term at frequency  $\omega$  of the incident light, which is usually negligible for asymmetric dipolar chromophores. However, for

some  $A_4$   $Zn^{II}$  porphyrins with a substituent in  $\beta$ -pyrrolic position, it was recently shown that this approximation cannot be made [21].

$\beta_{CT}$  and  $\beta_\lambda$  can be safely compared when the direction of the CT and of the dipole moment are almost coincident, as for 4-styrylpyridines axially coordinated to ZnTPP.

The purpose of the present research is to deepen the previous investigation [25] by considering from both an experimental and a theoretical point of view the impact that  $A_4$   $Zn^{II}$  porphyrin cores with different electron density might have on the second order NLO properties of 4-styrylpyridines bound in axial position.

As ligands, we have chosen an acceptor  $-NO_2$  (L1) and a donor  $-NMe_2$  group (L2) (Figure 1), equipped with a strong electron withdrawing  $-NO_2$  and a strong electron donor  $-NMe_2$  group, respectively. The arrows emphasize the direction conventionally assumed for the ground state dipole moment (from the negative to the positive pole of the molecule, Figure S1), which is opposite to the CT direction.

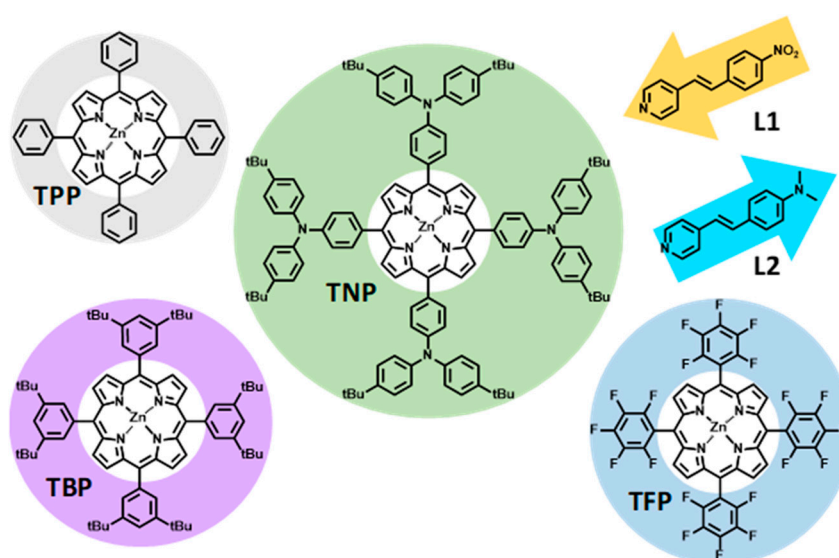


**Figure 1.** Molecular structures of  $Zn^{II}$  porphyrins and ligands.

In order to have a comprehensive understanding of the role of the metal complex, four  $A_4$   $Zn^{II}$  porphyrin cores with increasing electron density were selected (Figure 1). More in detail, the  $Zn^{II}$  porphyrins display in 5,10,15,20 *meso* position aryl moieties with remarkable electron acceptor properties (pentafluorophenyl (TFP)), and with moderate to strong electron donor properties (phenyl (TPP) < 3,5-di-*tert*-butylphenyl (TBP) < bis(4-*tert*-butylphenyl)anilines) (TNP)).

L1 and L2 have been coordinated to all the four porphyrin cores, and their EFISH quadratic hyperpolarizabilities  $\beta_\lambda$  have been compared to the Density Functional Theory (DFT)-calculated scalar quantities  $\beta_{||}$ , which derive from the full  $\beta$  tensor and correspond to 3/5 times  $\beta_\lambda$  ( $\beta_{||} = (3/5) \sum_i (\mu_i \beta_i) / \mu$ , where  $\beta_i = (1/5) \sum_j (\beta_{ijj} + \beta_{jij} + \beta_{jji})$ ) [29]. Our combined experimental and theoretical approach sheds light on the different interactions involved in the second order response of L1 and L2 axially coordinated to  $A_4$   $Zn^{II}$  porphyrins, suggesting a role of backdonation-type interactions in the determination of the negative sign of EFISH  $\beta_\lambda$ , and a not negligible third order contribution to the second order NLO response for L1-substituted complexes.

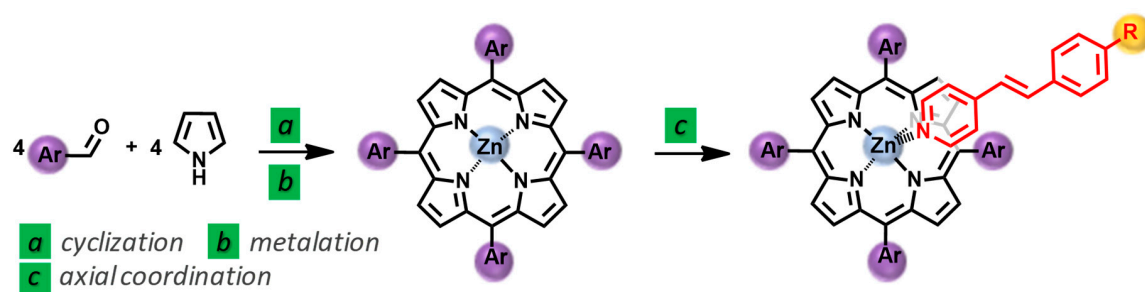
## 2. Results and Discussion

### 2.1. Synthesis of L1 and L2 Axially Substituted $A_4$ $Zn^{II}$ Porphyrins

The fabrication of push–pull porphyrin systems showing a *meso*-substitution pattern on 5,15-positions is commonly known far from being trivial. Indeed, the asymmetric 10,20-diaryl

substituted porphyrin core requires two reaction steps to be achieved and the further insertion of electron-donating and accepting pendants in 5,15-*meso* positions involves a tedious multistep pathway [30]. Instead, the  $\beta$ -pyrrolic substituted porphyrins, consisting of a more symmetric tetraaryl-substituted porphyrin core, are promptly accessible through a one-pot cyclo-condensation step among pyrrole and selected aldehydes [31,32]. However, the functionalization of  $\beta$ -pyrrolic positions and the subsequent introduction of proper substituents complicates the synthetic route [33,34].

Since the synthetic strategy of axially coordinated porphyrins is of a great value, the poor interest devoted on such class of porphyrins is quite surprising. Their fabrication relies on a less demanding synthetic strategy than that of  $\beta$ - and *meso*-substituted porphyrins by involving three effective and straightforward steps (Scheme 1): (a) cyclization of the core; (b) metalation; (c) axial coordination of metal center with proper ligands. As for  $\beta$ -pyrrolic substituted derivatives, the symmetric tetraaryl-substituted porphyrin core is easily attainable. Further, the coordination metals are typically inserted in the tetrapyrrolic core to quantitatively yield the desired metal complex. Finally, proper ligands can be successfully connected to the metal porphyrins by a simple axial-coordination step.



**Scheme 1.** Schematic synthetic pathway for the preparation of  $A_4 Zn^{II}$  porphyrins axially coordinated with 4-styrylpyridine ligands.

Except **TPP**, which was purchased from chemical vendors, the investigated free-base porphyrins **TBP** [30] and **TFP** [35] were synthesized as reported elsewhere. The acid-catalyzed Lindsey method [36] to prepare a porphyrin ring from aldehyde and pyrrole was adapted to the desired macrocycles. The following metalation step quantitatively determined the  $Zn^{II}$ -complexes by refluxing the corresponding free-base porphyrin with  $Zn(OAc)_2$  in  $CHCl_3$ . **TBP** was successfully obtained (43% yield) from pyrrole and 3,5-di-*tert*-butyl-benzaldehyde in  $CH_2Cl_2$  with trifluoroacetic acid (TFA) as catalyst and 2,3-dichloro-5,6-dicyano-1,4-benzoquinone (DDQ) as oxidant before undergoing a metalation step [30]. **TFP** synthesis instead required a  $BF_3 \cdot OEt_2$ -catalyst in anhydrous  $CH_2Cl_2$  to enable the condensation between pyrrole and pentafluorobenzaldehyde, and refluxing the solution with 2,3-dichloro-5,6-dicyano-1,4-benzoquinone (DDQ) to oxidize the macrocyclic ring (61% yield) before the subsequent zinc complexation [35,37]. Unlike **TBP** and **TFP** porphyrins, **TNP** nucleus was only obtained as  $Zn$ -complex from the following preparation strategy. A first cyclization step from *p*-bromobenzaldehyde and pyrrole yielded the *p*-bromophenyl substituted porphyrin core which was subsequently coordinated with a  $Zn^{II}$  metal ion. A multiple Buchwald–Hartwig amination of the resulting metal-porphyrin successfully provided the  $Zn$ TNP metal complex [38].

While the electron-donating ligand **L2** was purchased, the electron-accepting ligand **L1** was designed and synthesized with the purpose of combining their electronic effect with the above-mentioned electron-deficient and electron-rich porphyrins. **L1** was obtained by adapting an elsewhere reported procedure for similar stilbazole-based ligands [10] (see Supporting Information). Finally, **L1** and **L2** were coupled with the four  $Zn^{II}$ porphyrins **TPP**, **TBP**, **TNP**, and **TFP** by refluxing  $CH_2Cl_2$  solutions of the proper components from 3 h to 72 h depending on the specific combinations between porphyrin and ligands.

Axial coordination enabled to address the main issues related to the poor overall reaction yields of fabrication of porphyrins with more complicated architectures. The synthetic efforts indeed were largely

reduced by overcoming the more sensitive steps, namely, the functionalization and the subsequent covalent bonds formation at the periphery of porphyrin rings.

Thus, the trivial structural engineering demands of axially coordinated porphyrins allowed us to provide a prompt access to a large array of chromophores, offering a reasonable basis for a comprehensive screening of their NLO properties.

## 2.2. <sup>1</sup>H-NMR and UV-Vis Spectroscopy

The <sup>1</sup>H-NMR spectra of the axially substituted A<sub>4</sub> Zn<sup>II</sup> porphyrins show a remarkable shielding effect for the protons in  $\alpha$ -position of the pyridine nitrogen atom of the ligand, due to the local magnetic cone produced by the anisotropic interaction of the  $\pi$ -conjugated system of the porphyrin core with the magnetic field. For example, for free **L1** in CDCl<sub>3</sub>, they are at 8.59 ppm (Figure S2), and they downshift to 3.74 for **ZnTPP-L1** (Figure S3), 4.39 ppm for **ZnTBP-L1** (Figure S4), and 2.44 ppm for **ZnTFP-L1** (Figure S5). A comparable shift was reported for the axial coordination to ZnTPP of a ligand analogous to **L1**, but with a -CF<sub>3</sub> instead of a -NO<sub>2</sub> group (4.43 ppm) [25].

Moreover, the <sup>1</sup>H-NMR spectra show that the axial coordination of the 4-styrylpyridine to the porphyrin occurs with retention of the (*E*)-configuration of the double bond of the ligand. Indeed, the coupling constant between the olefinic hydrogens is 16.0 Hz, as expected for a *trans* arrangement.

Finally, some <sup>1</sup>H-NMR signals appear broadened, as typically observed after complexation of *free-base* porphyrins with metals and with the axial coordination of pyridine ligands [39].

We investigated **L1**, **L2**, and the axially coordinated Zn<sup>II</sup> porphyrins by UV-Vis absorption spectroscopy. The spectra in CHCl<sub>3</sub> solution are reported in the Supporting Information (Figures S6–S10), while the corresponding experimental data are summarized in Table 1.

**Table 1.** Electronic absorption data in CHCl<sub>3</sub> solution of ligands acceptor -NO<sub>2</sub> (**L1**) and donor -NMe<sub>2</sub> (**L2**) and of the axially coordinated A<sub>4</sub> Zn<sup>II</sup> porphyrins.

Compound	Ligand Band $\lambda_{\max}$ (nm)	Soret or B Band $\lambda_{\max}$ (nm)	Q <sub>IV</sub> Band $\lambda_{\max}$ (nm)	Q <sub>III</sub> Band $\lambda_{\max}$ (nm)	Q <sub>II</sub> Band $\lambda_{\max}$ (nm)	Q <sub>I</sub> Band $\lambda_{\max}$ (nm)
<b>L1</b>	332					
<b>L2</b>	376					
<b>TFP</b>		412	506	583	637	657
<b>ZnTFP</b>		419		551	584	
<b>ZnTFP-L1</b>	321	419		551	585	627
<b>ZnTFP-L2</b>		419	480	550	585	617
<b>TPP</b>		418	515	550	589	646
<b>ZnTPP</b>		422		553	594	
<b>ZnTPP-L1</b>	319	421		553	594	
<b>ZnTPP-L2</b>		422		553	594	
<b>TBP</b>		421	518	554	592	648
<b>ZnTBP</b>		424		552	595	
<b>ZnTBP-L1</b>	329	424		552	595	
<b>ZnTBP-L2</b>	372	424		552	595	
<b>ZnTNP</b>	306	438		559	605	
<b>ZnTNP-L1</b>	310	433		559	603	
<b>ZnTNP-L2</b>	305	434		559	603	

**L1** and **L2** show one electronic absorption band due to a  $\pi \rightarrow \pi^*$  internal transition for the former, whereas a  $n \rightarrow \pi^*$  ILCT transition from the -NMe<sub>2</sub> donor end to the pyridine ring for the latter [10,40,41].

The UV-Vis spectra of the free porphyrins and of the corresponding Zn<sup>II</sup> complexes display the typical pattern expected on the basis of the Gouterman's "four orbital model" [42]: an intense ( $\epsilon \sim 10^5 \text{ M}^{-1} \text{ cm}^{-1}$ ) Soret or B band at about 412–440 nm, due to the S<sub>0</sub>→S<sub>2</sub> transition (from the ground to the second excited state), and four (for free bases) or two (for the Zn<sup>II</sup> complexes) weaker ( $\epsilon \sim 10^4 \text{ M}^{-1} \text{ cm}^{-1}$ ) Q bands in the range 500–660 nm, due to S<sub>0</sub>→S<sub>1</sub> transitions (from the ground to

the first excited state). The complexation to the metal ion induces a slight bathochromic shift of the B band (3–7 nm;  $168\text{--}406\text{ cm}^{-1}$ ). A similar red shift occurs for the  $Q_{III}$  and  $Q_{II}$  bands in **ZnTPP** and for the  $Q_{II}$  band in **ZnTBP**. Conversely, for the electron-poor **TFP** core, the  $Q_{III}$  and  $Q_{II}$  bands experience a remarkable hypsochromic shift (30–50 nm;  $996\text{--}1425\text{ cm}^{-1}$ ) after complexation to  $\text{Zn}^{II}$ .

Despite the reported red shift of the B and particularly of the Q bands in a **ZnTPP** series with donor moieties in axial position [43,44], the UV–Vis spectra of the axially substituted  $\text{Zn}^{II}$  porphyrins investigated here match those of the unsubstituted complexes. **ZnTNP-L1** and **ZnTNP-L2** are exceptions since they show a slight blue shift of the B (4–5 nm;  $210\text{--}264\text{ cm}^{-1}$ ) and of the  $Q_{II}$  (2 nm;  $55\text{ cm}^{-1}$ ) band in comparison to **ZnTNP**.

When a 4-styrylpyridine is coordinated in axial position of a metal porphyrin, three possible interactions can occur (Figure 2): (i) an axial  $\sigma$ -donation from the pyridine nitrogen atom to the metal center, when R is a donor group [26]; (ii) an axial  $\pi$ -backdonation from the  $d_{\pi}$  orbitals of the metal to the  $\pi^*$  antibonding orbitals of the 4-styrylpyridine ligand, when R is an acceptor group [26]; and (iii) a peripheral  $\pi$ -backdonation from the  $d_{\pi}$  orbitals of the metal to the  $\pi^*$  orbitals of the porphyrin ring [43,44].

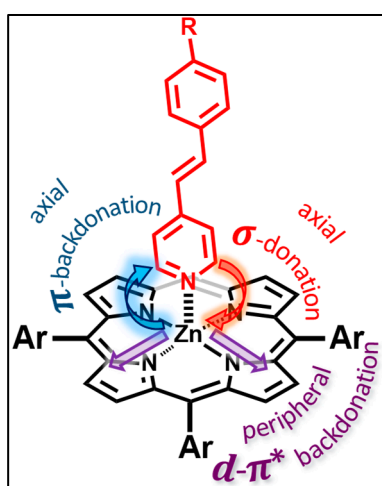


**Figure 2.** Possible interactions in axially substituted metal porphyrins.

When R is a donor group,  $\sigma$ -donation prevails with an accumulation of electron density on the metal center, which can be dissipated from the metal to the porphyrin core through *peripheral*  $d\text{-}\pi^*$  backdonation. As a result, a red shift of the absorption spectrum of the axially substituted metal porphyrin is expected in comparison to the unsubstituted one [43,44]. The lack of such a bathochromic shift in the spectra of our axial complexes suggests a significant role of the *axial*  $\pi$ -backdonation from  $\text{Zn}^{II}$  to the ligand, thanks to the energetically available  $\pi^*$  antibonding orbitals of the 4-styrylpyridine. Therefore, the competition between peripheral and axial backdonation flattens out any spectroscopic effect that an axial coordination may produce.

### 2.3. Experimental and Theoretical Investigation of the Second Order NLO Properties

We performed EFISH measurements of **L1**, **L2**, and of the axially substituted  $A_4\text{Zn}^{II}$  porphyrins on a  $10^{-3}\text{ M}$  solution in  $\text{CHCl}_3$  with a 1907 nm incident wavelength. Ground state dipole moments ( $\mu_0$ ) and  $\beta_{||}$  (that is equal to  $3/5\beta_{1907}$ ) were computed by Density Functional Theory (DFT) and Coupled Perturbed DFT (CP-DFT) M06-2X/6-311G (d) calculations. The details on both methodologies are in the Materials and Methods Section, and Table 2 collects the data.

**Table 2.** Experimental Electric-Field-Induced Second Harmonic generation (EFISH)  $\mu_0\beta_{1907}$  values ( $10^{-3}$  M solution in  $\text{CHCl}_3$ ), and theoretical  $\mu_0$  and  $\beta_{\parallel}$  values of ligands **L1** and **L2** and of the axially coordinated  $\text{A}_4$   $\text{Zn}^{\text{II}}$  porphyrins.

Compound	$\mu_0\beta_{1907}$ ( $\times 10^{-48}$ esu)	$\mu_{0 \text{ calc}}$ ( $\mu_0$ EF <sup>a</sup> ) (D)	$\beta_{1907}$ ( $\beta_{1907}$ EF <sup>b</sup> ) ( $\times 10^{-30}$ esu)	$\beta_{\parallel}$ ( $\beta_{\parallel}$ EF <sup>d</sup> ) ( $\times 10^{-48}$ esu)
<b>L1</b>	+310	2.67	+116	11
<b>ZnTFP-L1</b>	-1680	0.29	nd <sup>c</sup>	-3
<b>ZnTPP-L1</b>	-540	0.36	nd	7
<b>ZnTBP-L1</b>	-880	0.68	nd	7
<b>ZnTNP-L1</b>	-733	0.70	nd	12
<b>L2</b>	+250	6.59	+38 <sup>d</sup>	37
<b>ZnTFP-L2</b>	-980	10.63 (1.61)	-92 (2.42)	75 (2.0)
<b>ZnTPP-L2</b>	-280	9.84 (1.49)	-28 (0.74)	65 (1.75)
<b>ZnTBP-L2</b>	-860	9.64 (1.46)	-89 (2.34)	64 (1.73)
<b>ZnTNP-L2</b>	-606	9.31 (1.41)	-65 (1.71)	60 (1.62)

<sup>a</sup>  $\mu_0$  EF =  $\mu_{0,\text{complex}}/\mu_{0,\text{L2}}$ . <sup>b</sup>  $\beta_{1907}$  EF =  $\beta_{1907,\text{complex}}/\beta_{1907,\text{L2}}$ . <sup>c</sup> nd = not determined. <sup>d</sup>  $\beta_{1907}$  =  $+35 \times 10^{-30}$  esu from Reference [10]. <sup>d</sup>  $\beta_{\parallel}$  EF =  $\beta_{\parallel,\text{complex}}/\beta_{\parallel,\text{L2}}$ .

It should be noted that  $\mu_0$  of **L1** is significantly greater than that computed, at the same level of the theory, for the previously investigated 4-styrylpyridine carrying a  $-\text{CF}_3$  instead of a  $-\text{NO}_2$  group [10] equal to 0.44 D. Moreover, the dipole of **L2** is comparable to the one previously obtained by HF/6-311++G\*\* calculations (6.06 D) [4].

Upon coordination to the axial position of the  $\text{Zn}^{\text{II}}$  porphyrins, an increase of the  $\mu_0$  value of **L2** occurs, with enhancement factors ( $\mu_0$  EF =  $\mu_{0,\text{complex}}/\mu_{0,\text{ligand}}$ ) in the range of 1.41–1.61. The computed  $\mu_0$  are substantially the same regardless of the porphyrin core, suggesting that, when the  $\sigma$ -donation by the donor-substituted 4-styrylpyridine is remarkable, the core acts as a buffer of the metal ion electron density through the peripheral d- $\pi^*$  backdonation mechanism (Figure 2). Accordingly, a closer look at the axial complexes with **L2** shows that the  $\mu_0$  and  $\mu_0$  EF values follow the trend based on the different electron properties imparted to the porphyrin macrocycles by the substituents in 5,10,15,20 *meso* positions. As the core becomes more electron-poor ( $\text{ZnTNP} < \text{ZnTBP} < \text{ZnTPP} < \text{ZnTFP}$ ), its ability to dissipate the metal ion electron density by peripheral backdonation increases slightly, pushing up  $\mu_0$  and  $\mu_0$  EF.

On the other hand, when **L1** is coordinated to the axial position of the  $\text{Zn}^{\text{II}}$  porphyrins, the  $\mu_0$  values experience a huge decrease and essentially vanish for all the compounds. This is quite surprising since for the ligand similar to **L1**, carrying a  $-\text{CF}_3$  instead of a  $-\text{NO}_2$  acceptor group, coordination to ZnTPP led to a remarkable increase of  $\mu_0$  [25]. Apparently, in the present case, the higher electron acceptor properties of the  $-\text{NO}_2$  moiety (Hammett  $\sigma_{\text{para}} = 0.78$  vs. 0.54 for  $-\text{CF}_3$ ) [45] result into the quasi-cancellation of the ground state dipole moment of the axially coordinated Zn porphyrins. This could be ascribed to the axial  $\pi$ -backdonation from the metal towards the pyridinic nitrogen atom (see Figure 1), counteracting the polarity (from  $-\text{NO}_2$  to  $\text{N}_{\text{py}}$ ) of the free ligand in the same way as described for 4-nitropyridine-1-oxide in comparison to 4-nitropyridine [46]. The  $\mu_0$  of **ZnTFP-L1**, which is the lowest among the series, supports this hypothesis, since the pentafluorophenyl rings in *meso* position impart a significant electron depletion to the core, thus enhancing the Lewis acid properties of the  $\text{Zn}^{\text{II}}$  ion.

The axial coordination of **L2** to  $\text{Zn}^{\text{II}}$  porphyrins maintains and emphasizes the ground state charge distribution in agreement with an enhancement of the polarity (from  $\text{N}_{\text{py}}$  to  $-\text{NMe}_2$ ) in comparison to the free ligand. The opposite relative orientation of the ligands' dipole moment with respect to the metal-porphyrins reflects also into significantly different Zn- $\text{N}_{\text{py}}$  distances, which are longer by about 0.02 Å for the **L1**-complexes with respect to the **L2** ones (Table S1).

In agreement with the above considerations, the calculated  $\beta_{\parallel}$  values for **L2**-complexes are positive, because the second order NLO response of **L2** is dominated by a  $n \rightarrow \pi^*$  ILCT transition along the dipole

moment axis, which is enhanced by  $\sigma$  donation to the  $\text{Zn}^{\text{II}}$  porphyrin core. As expected [6], the  $\beta_{\parallel}$  value of **L2** increases upon coordination, with enhancement factors ( $\beta_{\parallel} \text{EF} = \beta_{\parallel, \text{complex}}/\beta_{\parallel, \text{ligand}}$ ) that are in the range of 1.62–2.0 and follow the trend of the  $\mu_0 \text{EF}$ .

On the other hand, in accordance with the quasi-null  $\mu_0$ , the values of  $\beta_{\parallel}$  computed for the  $\text{Zn}^{\text{II}}$  porphyrins with axially coordinated **L1** are very low and with no enhancement in comparison to the free ligand, as expected for a significant axial  $\pi$ -backdonation. Furthermore, when **L1** is in combination with ZnTFP, CP-DFT calculations provide a  $\beta_{\parallel}$  with a negative sign, associated with an inversion of the dipole moment direction thanks to the very electron-poor porphyrin core.

The experimental EFISH  $\beta_{1907}$  of **L1** and **L2** are positive, as expected, and the value recorded for **L2** is in nice agreement with the computed  $\beta_{\parallel}$  and with the experimental value already reported in the literature [10].

Conversely, all the axial porphyrins display a *negative* EFISH second order NLO response in accordance to the former research that reported a negative  $\beta_{\text{CT}}$  (provided by solvatochromism) for the coordination to ZnTPP of **L2** and of the ligand similar to **L1**, but with a  $-\text{CF}_3$  instead of a  $-\text{NO}_2$  group [25].

Since a negative value of  $\beta_{\text{CT}}$  (and of  $\beta_{1907}$ ) arises from a negative  $\Delta\mu_{\text{eg}}$  (Equation (1)), the CT transition mainly responsible for the second order NLO response of our  $\text{Zn}^{\text{II}}$  porphyrins with **L1** and **L2** in axial position leads to a decrease of the excited state dipole moment in comparison to the ground state one.

Thus, for **L2**-substituted complexes, we ought to assume that the key role in the determination of the *sign* of the EFISH response is played by the peripheral  $d-\pi^*$  backdonation (Figure 2), which favors a charge dissipation on the  $\pi$ -delocalized system of the porphyrin macrocycle, with a lowering of the dipole moment in the excited state. Moreover, our data confirm that no enhancement of the  $\beta_{1907}$  of **L2** occurs for coordination to ZnTPP (Table 2 and Reference [25]), whereas its second order NLO response increases when it is in axial position of the other  $\text{Zn}^{\text{II}}$  porphyrins, reaching the highest absolute value in combination to the most electron-poor core (**ZnTFP**). This is in agreement with an axial interaction mainly dominated by  $\sigma$ -donation, followed by peripheral backdonation, as discussed also for the dipole moments.

The interpretation of the high and negative  $\mu\beta_{1907}$  data for the axial complexes with **L1** is more intriguing. A low  $\mu_0$  is not inconsistent with a high quadratic hyperpolarizability, since the latter depends on  $\Delta\mu_{\text{eg}}$  (Equation (1)). Therefore, even when  $\mu_0$  is small, a high value of the excited state dipole moment is enough to reach a significant second order NLO response. However, when the  $\mu_0$  of the solute is negligible, the EFISH technique is hardly feasible.

Very recently, some of us reported a not negligible contribution to  $\gamma_{\text{EFISH}}$  of the third order term  $\gamma(-2\omega; \omega, \omega, 0)$  in Equation (2) for some  $\text{A}_4 \text{Zn}^{\text{II}}$  porphyrins with a substituent in  $\beta$ -pyrrolic position [21]. In particular, CP-DFT calculations provided large and negative  $\gamma_{\parallel}$  values ( $\gamma_{\parallel} = \gamma(-2\omega; \omega, \omega, 0)$ ) for two chromophores having  $\mu_0 = 0.6 \text{ D}$ , which is of the same order of magnitude as the ones of the **L1**-substituted axial porphyrins investigated here. Hence, we suggest that the EFISH second order NLO response of the latter might be affected by a significant and negative contribution of the electronic third order cubic term, which exceeds the value of the dipolar orientational contribution  $\mu_0\beta_{\lambda}/5kT$ . Therefore, apparently, coordination of a 4-stryrylpyridine with a strong electron withdrawing group in the axial position of an  $\text{A}_4 \text{Zn}^{\text{II}}$  porphyrin, being dominated by axial  $\pi$ -backdonation, leads to a quasi-null dipole moment, and therefore, to a chromophore with important third order properties. The very high value recorded for **ZnTFP-L1**, albeit the lowest dipole moment within the series, is unexpected and prompts us to deepen the present investigation with further DFT calculations and Third Harmonic Generation (THG) measurements, which will be the topic of another paper.



### 3. Materials and Methods

#### 3.1. General

All reagents and solvents were purchased from Sigma-Aldrich (Merck Life Science S.r.l., Milan, Italy) and used as received, except for  $\text{NEt}_3$  (freshly distilled over KOH) and  $\text{CH}_2\text{Cl}_2$  anhydrous for the synthesis of TFP (freshly distilled over  $\text{CaH}_2$ ). Milli-Q water was collected from the Millipore apparatus, equipped with 0.22  $\mu\text{m}$  filters. Glassware was flame-dried under vacuum before use when necessary. Microwave assisted reactions were performed using a Milestone Micro-SYNTH instrument (Milestone Srl, Sorisole, Italy). Silica gel for gravimetric chromatography (Geduran Si 60, 63–200  $\mu\text{m}$ ) and for flash chromatography (Kieselgel 60, 0.040–0.063 mm) were purchased from Merck (Merck KGaA, Darmstadt, Germany).  $^1\text{H-NMR}$  spectra were recorded on a Bruker AMX 300 and on a Bruker Avance DRX-400 (Bruker Italia S.r.l., Milan, Italy) in  $\text{CDCl}_3$  or in  $\text{THF-}d_8$  to enhance resolution (Cambridge Isotope Laboratories Inc., Tewksbury, MA, USA). Elemental analyses were carried out with a Perkin-Elmer CHN 2400 instrument in the Analytical Laboratories of the Department of Chemistry at the University of Milan. Electronic absorption spectra were recorded in  $\text{CHCl}_3$  solution at room temperature on a Shimadzu UV 3600 spectrophotometer (Shimadzu Corporation, Kyoto, Japan). The starting  $\text{A}_4 \text{Zn}^{\text{II}}$  porphyrin complexes were prepared as reported in literature [30]. The experimental details on the synthesis and characterization of the investigated axial compounds are reported in the Supplementary Materials.

#### 3.2. EFISH and THG Measurements

The second order NLO responses of the axially coordinated  $\text{A}_4 \text{Zn}^{\text{II}}$  porphyrins with **L1** and **L2** ligands were measured by the EFISH technique [27,28] in the Department of Chemistry of the University of Milano (Milano, Italy) through a prototype apparatus made by SOPRA (Paris, France). For each chromophore, measurements were performed on freshly prepared solutions in  $\text{CHCl}_3$  at  $10^{-3}$  M concentration. The 1907 nm laser incident wavelength was chosen because its second harmonic (at 953 nm) is far enough from the absorption bands of the chromophores to avoid possible enhancement of the second order NLO response due to resonance effects. The incident beam was obtained by Raman shifting of the 1064 nm emission of a Q-switched Nd:YAG laser in a high-pressure hydrogen cell (60 bar). A liquid cell with thick windows in the wedge configuration was used to obtain the Maker fringe pattern originated by the harmonic intensity variation as a function of the liquid cell translation. In the EFISH experiments, this incident beam was synchronized with a direct current field applied to the solution, with 60 and 20 ns pulse duration, respectively, in order to break its centrosymmetry. The comparison of the harmonic signal of the chromophore solution with that of the pure solvent allowed the determination of its second order NLO response (assumed to be real because the imaginary part was neglected). The  $\mu_0\beta_{1907}$  values reported in Table 2 are the mean values of 12 successive measurements performed on the same sample and are defined according to the “phenomenological” convention [47]. The experimental error on the EFISH measurements is 10–15%.

#### 3.3. Computational Calculations

Geometry optimizations were performed with the 6-311G(d) basis set using the M06 functional [48] due to its specific parametrization on organometallic complexes. Using the same basis set, SHG first hyperpolarizabilities, i.e., the  $\beta(-2\omega; \omega, \omega)$  tensors, were computed within the Coupled Perturbed Kohn–Sham (CPKS) approach at the same frequency (1907 nm) used in the EFISH experiments. The M06-2X functional [48], which has been recently recommended for hyperpolarizability calculations of mid-size chromophores [49], was adopted for  $\beta$  calculation. The same functional was used for determining the dipole moments  $\mu_0$ . A pruned (99,590) grid was selected for computation and use of two-electron integrals and their derivatives. To get a meaningful comparison with the experimental data, the scalar quantity  $\beta_{\parallel}$  was derived from the full tensors  $\beta$ ;  $\beta_{\parallel}$  corresponds to 3/5 times  $\beta_{\lambda}$ , the projection along the dipole moment direction of the vectorial component of the  $\beta$  tensor, that is

$\beta_{\parallel} = (3/5) \sum_i (\mu_i \beta_i) / \mu$ , where  $\beta_i = (1/5) \sum_j (\beta_{ijj} + \beta_{jij} + \beta_{jji})$  [29]. All Density Functional Theory (DFT) calculations were performed using the Gaussian16 suite of programs [50].

#### 4. Conclusions

Two 4-styrylpyridines carrying an electron acceptor  $-\text{NO}_2$  (**L1**) or an electron donor  $-\text{NMe}_2$  group (**L2**), respectively, were axially coordinated to  $\text{A}_4 \text{Zn}^{\text{II}}$  porphyrins with aryl moieties of increasing electron density in 5,10,15,20 *meso* position: pentafluorophenyl (**TFP**) < phenyl (**TPP**) < 3,5-di-*tert*-butylphenyl (**TBP**) < bis(4-*tert*-butylphenyl)aniline (**TNP**). The EFISH quadratic hyperpolarizabilities  $\beta_{\lambda}$  were measured and compared to the DFT-calculated scalar quantities  $\beta_{\parallel}$ . Our combined experimental and theoretical approach sheds light on the different interactions involved in the second order response of **L1** and **L2** axially coordinated to  $\text{A}_4 \text{Zn}^{\text{II}}$  porphyrins, suggesting a role of backdonation-type interactions in the determination of the negative sign of EFISH  $\beta_{\lambda}$ , and a not negligible third order contribution to the second order NLO response for **L1**-substituted complexes.

An increase of the ground state dipole moment of **L2** occurs upon coordination, and the computed  $\mu_0$  values are the same regardless of the macrocycle, suggesting a remarkable axial  $\sigma$ -donation from the pyridine nitrogen atom to the metal center, with an accumulation of electron density on this latter, which can be dissipated through a peripheral metal  $\rightarrow$  porphyrin  $d_{\pi}-\pi^*$  backdonation.

On the other hand, when **L1** is coordinated to the axial position of the  $\text{Zn}^{\text{II}}$  porphyrins, the  $\mu_0$  values essentially vanish, as expected for a significant axial  $\pi$ -backdonation from the metal towards the pyridine nitrogen atom, counteracting the polarity (from  $-\text{NO}_2$  to  $\text{N}_{\text{py}}$ ) of the free ligand.

In accordance, the computed  $\beta_{\parallel}$  for **L2** and the corresponding axial complexes are positive, with an enhancement upon coordination, while the quasi-null  $\mu_0$  of the  $\text{Zn}^{\text{II}}$  porphyrins with **L1** produces very low  $\beta_{\parallel}$  values and with no enhancement in comparison to the free ligand. Moreover, when **L1** is in combination with the most electron-poor core of the series (**ZnTFP**), CP-DFT calculations provide a  $\beta_{\parallel}$  with a negative sign.

The EFISH measurements confirm a positive  $\beta_{1907}$  for **L1** and **L2**, whereas all the axial porphyrins display a *negative* second order NLO response in accordance to the negative  $\beta_{\text{CT}}$  reported in a previous research for the coordination to **ZnTPP** of **L2** and of the ligand similar to **L1**, but with a  $-\text{CF}_3$  instead of a  $-\text{NO}_2$  group [26]. Hence, we suggest that for **L2**-substituted complexes, the key role in the determination of the sign of the EFISH response is played by the peripheral  $d-\pi^*$  backdonation, which leads to a decrease of the excited state dipole moment in comparison to the ground state one.

For **L1**-substituted complexes, the striking contrast between the almost vanishing  $\mu_0$  and the high and negative  $\mu\beta_{1907}$  data prompts us to suggest that the EFISH second order NLO response might be affected by a significant and negative contribution of the electronic third order cubic term  $\gamma(-2\omega; \omega, \omega, 0)$  to  $\gamma_{\text{EFISH}}$ , overwhelming the dipolar orientational contribution  $\mu_0\beta_{\lambda}/5kT$ . Therefore, apparently, the coordination of a 4-styrylpyridine with a strong electron withdrawing group in the axial position of an  $\text{A}_4 \text{Zn}^{\text{II}}$  porphyrin, being dominated by axial  $\pi$ -backdonation, originates a chromophore with important third order properties.

**Supplementary Materials:** The following are available online at <http://www.mdpi.com/2304-6740/8/8/45/s1>: the synthesis and characterization of **L1** and of the axially substituted  $\text{Zn}^{\text{II}}$  porphyrins; the  $^1\text{H-NMR}$  spectra; the UV-Vis spectra in  $\text{CHCl}_3$  solution; the optimized geometry of **L1** and **L2**; the computed distances between Zn and the pyridine nitrogen atoms.

**Author Contributions:** Conceptualization: F.T., G.D.C. and A.O.B.; Formal analysis: A.F.; Funding acquisition: G.D.C.; Investigation: F.T. and S.R.; Writing-original draft: F.T. and G.D.C.; Writing-review and editing: F.L. and A.O.B. All the authors have given approval to the final version of the manuscript. All authors have read and agreed to the published version of the manuscript.

**Funding:** This research was funded by the University of Milan (Piano Sostegno alla Ricerca 2018 LINEA 2 Azione A—Giovani Ricercatori).

**Acknowledgments:** We gratefully acknowledge Regione Lombardia and Fondazione Cariplo for the use of instrumentation purchased through the SmartMatLab Centre project (Fondazione Cariplo Grant 2013-1766).

**Conflicts of Interest:** The authors declare no conflict of interest.

## References

1. Di Bella, S. Second-order nonlinear optical properties of transition metal complexes. *Chem. Soc. Rev.* **2001**, *30*, 355–366. [[CrossRef](#)]
2. Cariati, E.; Pizzotti, M.; Roberto, D.; Tessore, F.; Ugo, R. Coordination and organometallic compounds and inorganic-organic hybrid crystalline materials for second-order non-linear optics. *Coord. Chem. Rev.* **2006**, *250*. [[CrossRef](#)]
3. Di Bella, S.; Dragonetti, C.; Pizzotti, M.; Roberto, D.; Tessore, F.; Ugo, R. *Molecular Organometallic Materials for Optics*; Springer: Berlin, Germany, 2010; Volume 28.
4. Roberto, D.; Ugo, R.; Bruni, S.; Cariati, E.; Cariati, F.; Fantucci, P.; Invernizzi, I.; Quici, S.; Ledoux, I.; Zyss, J. Quadratic hyperpolarizability enhancement of para-substituted pyridines upon coordination to organometallic moieties: The ambivalent donor or acceptor role of the metal. *Organometallics* **2000**, *19*, 1775–1788. [[CrossRef](#)]
5. Baccouche, A.; Peigné, B.; Ibersiene, F.; Hammoutène, D.; Boutarfâa, A.; Boucekkine, A.; Feuvrie, C.; Maury, O.; Ledoux, I.; Le Bozec, H. Effects of the metal center and substituting groups on the linear and nonlinear optical properties of substituted styryl-bipyridine metal(II) dichloride complexes: DFT and TDDFT computational investigations and harmonic light scattering measurements. *J. Phys. Chem. A* **2010**, *114*, 5429–5438. [[CrossRef](#)] [[PubMed](#)]
6. Roberto, D.; Ugo, R.; Tessore, F.; Lucenti, E.; Quici, S.; Vezza, S.; Fantucci, P.; Invernizzi, I.; Bruni, S.; Ledoux-Rak, I.; et al. Effect of the Coordination to M(II) Metal Centers (M = Zn, Cd, Pt) on the Quadratic Hyperpolarizability of Various Substituted 5-X-1,10-phenanthrolines (X Donor Group) and of trans-4-(Dimethylamino)-4'-stilbazole. *Organometallics* **2002**, *21*. [[CrossRef](#)]
7. Roberto, D.; Tessore, F.; Ugo, R.; Bruni, S.; Manfredi, A.; Quici, S. Terpyridine Zn(II), Ru(III) and Ir(III) complexes as new asymmetric chromophores for nonlinear optics: First evidence for a shift from positive to negative value of the quadratic hyperpolarizability of a ligand carrying an electron donor substituent upon. *Chem. Commun.* **2002**, *2*, 846–847. [[CrossRef](#)]
8. Tessore, F.; Roberto, D.; Ugo, R.; Pizzotti, M.; Quici, S.; Cavazzini, M.; Bruni, S.; De Angelis, F. Terpyridine Zn(II), Ru(III), and Ir(III) complexes: The relevant role of the nature of the metal ion and of the ancillary ligands on the second-order nonlinear response of terpyridines carrying electron donor or electron acceptor groups. *Inorg. Chem.* **2005**, *44*. [[CrossRef](#)]
9. Kanis, D.R.; Lacroix, P.G.; Ratner, M.A.; Marks, T.J. Electronic Structure and Quadratic Hyperpolarizabilities in Organotransition-Metal Chromophores Having Weakly Coupled  $\pi$ -Networks. Unusual Mechanisms for Second-Order Response. *J. Am. Chem. Soc.* **1994**, *116*, 10089–10102. [[CrossRef](#)]
10. Lucenti, E.; Cariati, E.; Dragonetti, C.; Manassero, L.; Tessore, F. Effect of the coordination to the “Os<sub>3</sub>(CO)<sub>11</sub>” cluster core on the quadratic hyperpolarizability of trans-4-(4'-X-styryl)pyridines (X = NMe<sub>2</sub>, t-Bu, CF<sub>3</sub>) and trans,trans-4-(4'-NMe<sub>2</sub>-phenyl-1,3-butadienyl). *Organometallics* **2004**, *23*. [[CrossRef](#)]
11. Oudar, J.L. Optical nonlinearities of conjugated molecules. Stilbene derivatives and highly polar aromatic compounds. *J. Chem. Phys.* **1977**, *67*, 446–457. [[CrossRef](#)]
12. Oudar, J.L.; Chemla, D.S. Hyperpolarizabilities of the nitroanilines and their relations to the excited state dipole moment. *J. Chem. Phys.* **1977**, *66*, 2664–2668. [[CrossRef](#)]
13. Bruni, S.; Cariati, E.; Cariati, F.; Porta, F.A.; Quici, S.; Roberto, D. Determination of the quadratic hyperpolarizability of trans-4-[4-(dimethylamino)styryl]pyridine and 5-dimethylamino-1,10-phenanthroline from solvatochromism of absorption and fluorescence spectra: A comparison with the electric-field-induced second-harmon. *Spectrochim. Acta Part A Mol. Biomol. Spectrosc.* **2001**, *57*, 1417–1426. [[CrossRef](#)]
14. Pizzotti, M.; Annoni, E.; Ugo, R.; Bruni, S.; Quici, S.; Fantucci, P.; Bruschi, M.; Zerbi, G.; Zoppo, M. Del A multitechnique investigation of the second order NLO response of a 10,20-diphenylporphyrinato nickel(II) complex carrying a phenylethynyl based push-pull system in the 5- and 15-positions. *J. Porphyr. Phthalocyanines* **2004**, *8*, 1311–1324. [[CrossRef](#)]
15. Morotti, T.; Pizzotti, M.; Ugo, R.; Quici, S.; Bruschi, M.; Mussini, P.; Righetto, S. Electronic characterisation and significant second-order NLO response of 10,20-diphenylporphyrins and their Zn<sup>II</sup> complexes substituted in the meso position with  $\pi$ -delocalised linkers carrying push or pull groups. *Eur. J. Inorg. Chem.* **2006**, 1743–1757. [[CrossRef](#)]

16. De Angelis, F.; Fantacci, S.; Sgamellotti, A.; Pizzotti, M.; Tessore, F.; Orbelli Biroli, A. Time-dependent and coupled-perturbed DFT and HF investigations on the absorption spectrum and non-linear optical properties of push-pull M(II)-porphyrin complexes (M = Zn, Cu, Ni). *Chem. Phys. Lett.* **2007**, *447*, 10–15. [[CrossRef](#)]
17. Pizzotti, M.; Tessore, F.; Orbelli Biroli, A.; Ugo, R.; De Angelis, F.; Fantacci, S.; Sgamellotti, A.; Zuccaccia, D.; Macchioni, A. An EFISH, theoretical, and PGSE NMR investigation on the relevant role of aggregation on the second order response in CHCl<sub>3</sub> of the push-pull chromophores [5-[[4'-(dimethylamino)phenyl]ethynyl]-15-[[4''-nitrophenyl]ethynyl]-10,20diphenylporphyrin]. *J. Phys. Chem. C* **2009**, *113*. [[CrossRef](#)]
18. Orbelli Biroli, A.; Tessore, F.; Righetto, S.; Forni, A.; Macchioni, A.; Rocchigiani, L.; Pizzotti, M.; Di Carlo, G. Intriguing Influence of –COOH-Driven Intermolecular Aggregation and Acid-Base Interactions with *N,N*-Dimethylformamide on the Second-Order Nonlinear-Optical Response of 5,15 Push-Pull Diarylzinc(II) Porphyrinates. *Inorg. Chem.* **2017**, *56*. [[CrossRef](#)]
19. Annoni, E.; Pizzotti, M.; Ugo, R.; Quici, S.; Morotti, T.; Bruschi, M.; Mussini, P. Synthesis, electronic characterisation and significant second-order non-linear optical responses of *meso*-tetraphenylporphyrins and their Zn<sup>II</sup> complexes carrying a push or pull group in the β pyrrolic position. *Eur. J. Inorg. Chem.* **2005**, 3857–3874. [[CrossRef](#)]
20. Tessore, F.; Orbelli Biroli, A.; Di Carlo, G.; Pizzotti, M. Porphyrins for Second Order Nonlinear Optics (NLO): An Intriguing History. *Inorganics* **2018**, *6*, 81. [[CrossRef](#)]
21. Di Carlo, G.; Pizzotti, M.; Righetto, S.; Forni, A.; Tessore, F. Electric-Field-Induced Second Harmonic Generation Nonlinear Optic Response of A4 β-Pyrrolic-Substituted Zn<sup>II</sup> Porphyrins: When Cubic Contributions Cannot Be Neglected. *Inorg. Chem.* **2020**, *59*, 7561–7570. [[CrossRef](#)]
22. Bajju, G.D.; Kundan, S.; Kapahi, A.; Gupta, D. Synthesis and Spectroscopic Studies of Axially Ligated Zn(II)5,10,15,20-*meso*-tetra(p-chlorophenyl)porphyrin with Oxygen and Nitrogen Donors. *J. Chem.* **2013**, *2013*, 135815. [[CrossRef](#)]
23. Charisiadis, A.; Stangel, C.; Nikolaou, V.; Roy, M.S.; Sharma, G.D.; Coutsolelos, A.G. A supramolecular assembling of zinc porphyrin with a π-conjugated oligo(phenylenevinylene) (oPPV) molecular wire for dye sensitized solar cell. *Rsc Adv.* **2015**, *5*, 88508–88519. [[CrossRef](#)]
24. Xie, M.; Bai, F.-Q.; Zhang, H.-X.; Zheng, Y.-Q. The influence of an inner electric field on the performance of three types of Zn-porphyrin sensitizers in dye sensitized solar cells: A theoretical study. *J. Mater. Chem. C* **2016**, *4*, 10130–10145. [[CrossRef](#)]
25. Annoni, E.; Pizzotti, M.; Ugo, R.; Quici, S.; Morotti, T.; Casati, N.; Macchi, P. The effect on E-stilbazoles second order NLO response by axial interaction with M(II) 5,10,15,20-tetraphenyl porphyrinates (M = Zn, Ru, Os); a new crystalline packing with very large holes. *Inorg. Chim. Acta* **2006**, *359*, 3029–3041. [[CrossRef](#)]
26. Cole, S.J.; Curthoys, G.C.; Magnusson, E.A. Ligand Binding by Metalloporphyrins. I. Thermodynamic Functions of Porphyriniron(II)-Pyridine Complexes. *J. Am. Chem. Soc.* **1970**, *92*, 2991–2996. [[CrossRef](#)]
27. Levine, B.F.; Bethea, C.G. Molecular hyperpolarizabilities determined from conjugated and nonconjugated organic liquids. *Appl. Phys. Lett.* **1974**, *24*, 445–447. [[CrossRef](#)]
28. Singer, K.D.; Garito, A.F. Measurements of molecular second order optical susceptibilities using dc induced second harmonic generation. *J. Chem. Phys.* **1981**, *75*, 3572–3580. [[CrossRef](#)]
29. Kurtz, H.A.; Dudas, D.S. Quantum mechanical methods for predicting nonlinear optical properties. In *Reviews in Computational Chemistry*; 2007; Volume 12, pp. 241–279. [[CrossRef](#)]
30. Di Carlo, G.; Orbelli Biroli, A.; Pizzotti, M.; Tessore, F.; Trifiletti, V.; Ruffo, R.; Abboto, A.; Amat, A.; De Angelis, F.; Mussini, P.R. Tetraaryl Zn<sup>II</sup> porphyrinates substituted at β-pyrrolic positions as sensitizers in dye-sensitized solar cells: A comparison with *meso*-disubstituted push-pull Zn<sup>II</sup> porphyrinates. *Chem. A Eur. J.* **2013**, *19*, 10723–10740. [[CrossRef](#)]
31. Di Carlo, G.; Orbelli Biroli, A.; Tessore, F.; Caramori, S.; Pizzotti, M. β-Substituted Zn<sup>II</sup> porphyrins as dyes for DSSC: A possible approach to photovoltaic windows. *Coord. Chem. Rev.* **2018**, *358*, 153–177. [[CrossRef](#)]
32. Di Carlo, G.; Orbelli Biroli, A.; Pizzotti, M.; Tessore, F. Efficient sunlight harvesting by A4 β-Pyrrolic Substituted Zn<sup>II</sup> Porphyrins: A Mini-Review. *Front. Chem.* **2019**, *7*. [[CrossRef](#)]
33. Di Carlo, G.; Caramori, S.; Casarin, L.; Orbelli Biroli, A.; Tessore, F.; Argazzi, R.; Oriana, A.; Cerullo, G.; Bignozzi, C.A.; Pizzotti, M. Charge Transfer Dynamics in β and Meso Substituted Dithienylethylene Porphyrins. *J. Phys. Chem. C* **2017**, *121*, 18385–18400. [[CrossRef](#)]

34. Di Carlo, G.; Orbelli Biroli, A.; Tessore, F.; Rizzato, S.; Forni, A.; Magnano, G.; Pizzotti, M. Light-Induced Regiospecific Bromination of meso-Tetra(3,5-di-tert-butylphenyl)Porphyrin on 2,12  $\beta$ -Pyrrolic Positions. *J. Org. Chem.* **2015**, *80*, 4973–4980. [[CrossRef](#)] [[PubMed](#)]
35. Orbelli Biroli, A.; Tessore, F.; Di Carlo, G.; Pizzotti, M.; Benazzi, E.; Gentile, F.; Berardi, S.; Bignozzi, C.A.; Argazzi, R.; Natali, M.; et al. Fluorinated Zn<sup>II</sup> Porphyrins for Dye-Sensitized Aqueous Photoelectrosynthetic Cells. *ACS Appl. Mater. Interfaces* **2019**, *11*, 32895–32908. [[CrossRef](#)] [[PubMed](#)]
36. Lindsey, J.S.; Schreiman, I.C.; Hsu, H.C.; Kearney, P.C.; Marguerettaz, A.M. Rothemund and Adler-Longo reactions revisited: Synthesis of tetraphenylporphyrins under equilibrium conditions. *J. Org. Chem.* **1987**, *52*, 827–836. [[CrossRef](#)]
37. Berardi, S.; Caramori, S.; Benazzi, E.; Zabini, N.; Niorettini, A.; Orbelli Biroli, A.; Pizzotti, M.; Tessore, F.; Di Carlo, G. Electronic Properties of Electron-Deficient Zn(II) Porphyrins for HBr Splitting. *Appl. Sci.* **2019**, *9*, 2739. [[CrossRef](#)]
38. Covezzi, A.; Orbelli Biroli, A.; Tessore, F.; Forni, A.; Marinotto, D.; Biagini, P.; Di Carlo, G.; Pizzotti, M. 4D- $\pi$ -1A type  $\beta$ -substituted Zn<sup>II</sup>-porphyrins: Ideal green sensitizers for building-integrated photovoltaics. *Chem. Commun.* **2016**, *52*. [[CrossRef](#)]
39. Shirazi, A.; Goff, H.M. Carbon-13 and Proton NMR Spectroscopy of Four- and Five-Coordinate Cobalt(II) Porphyrins: Analysis of NMR Isotropic Shifts. *Inorg. Chem.* **1982**, 3420–3425. [[CrossRef](#)]
40. Tessore, F.; Roberto, D.; Ugo, R.; Mussini, P.; Quici, S.; Ledoux-Rak, I.; Zyss, J. Large, concentration-dependent enhancement of the quadratic hyperpolarizability of [Zn(CH<sub>3</sub>CO<sub>2</sub>)<sub>2</sub>(L)<sub>2</sub>] in CHCl<sub>3</sub> on substitution of acetate by triflate. *Angew. Chem. Int. Ed.* **2003**, *42*. [[CrossRef](#)]
41. Tessore, F.; Locatelli, D.; Righetto, S.; Roberto, D.; Ugo, R.; Mussini, P. An Investigation on the Role of the Nature of Sulfonate Ancillary Ligands on the Strength and Concentration Dependence of the Second-Order NLO Responses in CHCl<sub>3</sub> of Zn(II) Complexes with 4,4'-*trans*-NC<sub>5</sub>H<sub>4</sub>CH=CHC<sub>6</sub>H<sub>4</sub>NMe<sub>2</sub> and 4,4'-*trans,trans*-NC<sub>5</sub>H<sub>4</sub>(CH=CH)<sub>2</sub>C<sub>6</sub>H<sub>4</sub>NMe<sub>2</sub>. *Inorg. Chem.* **2005**, *44*, 2437–2442.
42. Gouterman, M. Spectra of porphyrins. *J. Mol. Spectrosc.* **1961**, *6*, 138–163. [[CrossRef](#)]
43. Nappa, M.; Valentine, J.S. The Influence of Axial Ligands on Metalloporphyrin Visible Absorption Spectra. Complexes of Tetraphenylporphinatozinc. *J. Am. Chem. Soc.* **1978**, *100*, 5075–5080. [[CrossRef](#)]
44. Szintay, G.; Horváth, A. Temperature dependence study of five-coordinate complex formation of zinc(II) octaethyl and tetraphenylporphyrin. *Inorg. Chim. Acta* **2000**, *310*, 175–182. [[CrossRef](#)]
45. Hansch, C.; Leo, A.; Taft, R.W. A Survey of Hammett Substituent Constants and Resonance and Field Parameters. *Chem. Rev.* **1991**, *91*, 165–195. [[CrossRef](#)]
46. Zyss, J.; Chemla, D.S.; Nicoud, J.F. Demonstration of efficient nonlinear optical crystals with vanishing molecular dipole moment: Second-harmonic generation in 3-methyl-4-nitropyridine-1-oxide. *J. Chem. Phys.* **1981**, *74*, 4800–4811. [[CrossRef](#)]
47. Willetts, A.; Rice, J.E.; Burland, D.M.; Shelton, D.P. Problems in the comparison of theoretical and experimental hyperpolarizabilities. *J. Chem. Phys.* **1992**, *97*, 7590–7599. [[CrossRef](#)]
48. Zhao, Y.; Truhlar, D.G. The M06 suite of density functionals for main group thermochemistry, thermochemical kinetics, noncovalent interactions, excited states, and transition elements: Two new functionals and systematic testing of four M06-class functionals and 12 other function. *Theor. Chem. Acc.* **2008**, *120*, 215–241. [[CrossRef](#)]
49. Johnson, L.E.; Dalton, L.R.; Robinson, B.H. Optimizing calculations of electronic excitations and relative hyperpolarizabilities of electrooptic chromophores. *Acc. Chem. Res.* **2014**, *47*, 3258–3265. [[CrossRef](#)]
50. Frisch, M.J.; Trucks, G.W.; Schlegel, H.B.; Scuseria, G.E.; Robb, M.A.; Cheeseman, J.R.; Scalmani, G.; Barone, V.; Petersson, G.A.; Nakatsuji, H.; et al. *Gaussian 16*; revision, A.03; Gaussian, Inc.: Wallingford, CT, USA, 2016.

